HHS Public Access

Author manuscript

J Invest Dermatol. Author manuscript; available in PMC 2013 October 01.

Published in final edited form as:

J Invest Dermatol. 2013 April ; 133(4): 881–889. doi:10.1038/jid.2012.398.

Prostaglandin D_2 inhibits wound-induced hair follicle neogenesis through the receptor, *Gpr44*

Amanda M. Nelson[*,1], **Dorothy E. Loy**[*,4], **John A. Lawson**[2,3], **Adiya S. Katseff**[1], **Garret A. FitzGerald**[2,3], and **Luis A. Garza**[1]

[1]Department of Dermatology, Johns Hopkins University School of Medicine, Baltimore, MD

[2]Department of Pharmacology, University of Pennsylvania, Philadelphia, PA

[3]Institute for Translational Medicine and Therapeutics, University of Pennsylvania, Philadelphia, PA

[4]The University of Pennsylvania School of Medicine, Philadelphia, PA

Abstract

Prostaglandins (PGs) are key inflammatory mediators involved in wound healing and regulating hair growth; however, their role in skin regeneration after injury is unknown. Using wound-induced hair follicle neogenesis (WIHN) as a marker of skin regeneration, we hypothesized that PGD_2 decreases follicle neogenesis. PGE_2 and PGD_2 were elevated early and late respectively during wound healing. The levels of WIHN, lipocalin-type prostaglandin D_2 synthase (*Ptgds*) and its product PGD_2 each varied significantly among background strains of mice after wounding and all correlated such that the highest *Ptgds* and PGD_2 levels were associated with the lowest amount of regeneration. Additionally, an alternatively spliced transcript variant of *Ptgds* missing exon 3 correlated with high regeneration in mice. Exogenous application of PGD_2 decreased WIHN in wild type mice and PGD_2 receptor *Gpr44* null mice showed increased WIHN compared to strain-matched control mice. Furthermore, *Gpr44* null mice were resistant to PGD_2-induced inhibition of follicle neogenesis. In all, these findings demonstrate that PGD_2 inhibits hair follicle regeneration through the *Gpr44* receptor and imply that inhibition of PGD_2 production or *Gpr44* signaling will promote skin regeneration.

Corresponding Author: Luis A. Garza, MD, PhD., Assistant Professor of Dermatology, Department of Dermatology, Johns Hopkins University, School of Medicine, CRB II Suite 204, 1551 Orleans Street, Baltimore, MD 21231, USA, LAG@jhmi.edu, Phone: 410-614-6700, Fax: 410-614-0635.

*Authors contributed equally to this work

Author contributions:

AMN designed and performed research, analyzed data and wrote manuscript. DEL performed research and analyzed data. ASK performed research studies. LAG designed experiments and directed the project. JAL and GAF contributed reagents and performed sample analysis.

Conflict of Interest

The authors have no financial conflicts of interest.

Introduction

Scar formation and tissue regeneration are opposite results of the wound healing process. While fibrosis is more common after skin injury, full skin regeneration results in complete replacement of adnexa and function. Examples of tissue regeneration in mammalian systems include annual regeneration in deer antlers, ear regeneration following tag removal in mice and rabbits, and regeneration of amputated digit tips and liver regeneration in both mice and humans (Han *et al.*, 2005; Jia, ; Metcalfe *et al.*, 2006; Price *et al.*, 2005). In skin, Ito and Cotsarelis fully described and characterized *de novo* hair follicle neogenesis that is dependent on Wnt signaling after full-thickness wounding in mice. These regenerated hair follicles establish a stem cell population, express hair follicle-differentiation markers, produce a functional hair shaft, successfully transition through all phases of the hair cycle and include associated structures such as sebaceous glands (Ito *et al.*, 2007). However, what triggers mammalian regeneration is not completely understood. Determining which factors regulate this process may reveal mechanisms and lead to specifically-designed therapies to enhance regeneration.

Prostaglandins (PGs) are lipid signaling molecules enzymatically derived from arachidonic acid that function in both an autocrine and paracrine manner to regulate broad functions. Prostaglandin-endoperoxidase synthase 2 (Ptgs2; prostaglandin G/H synthase, cyclooxygenase 2 (Cox2)) is a key enzyme in the prostaglandin biosynthesis pathway, converting arachidonic acid to prostaglandin H_2, from which prostacyclin, thromboxane A2, PGD_2, PGE_2 and $PGF_{2\alpha}$ are produced by specific synthase enzymes. Individual PGs often have opposing biological effects. For example, in the lung, PGE_2 causes relaxation, while PGD_2 causes contraction of bronchial muscle (L. S. Goodman, 1996).

Recent studies demonstrate that PGs regulate hair growth. Increases in prostaglandin levels within the epidermis through overexpression of *Ptgs2* cause alopecia, sebaceous hyperplasia and may or may not cause a predisposition to squamous cell tumors (Bol *et al.*, 2002; Muller-Decker *et al.*, 1998; Neufang *et al.*, 2001). Prostaglandin D_2, E_2 and $F_{2\alpha}$ metabolism and signaling proteins are expressed in the hair follicle (Colombe *et al.*, 2007; Garza *et al.*, 2012). The FDA-approved $PGF_{2\alpha}$ analog, bimatoprost, is used clinically to enhance hair growth of human eyelashes (Johnstone and Albert, 2002). PGE_2 and $PGF_{2\alpha}$ enhance hair growth in mice (Geng *et al.*, 1992; Sasaki *et al.*, 2005). In contrast, PGD_2 inhibits hair growth in humans and mice (Garza *et al.*, 2012), demonstrating the opposing functions of prostaglandins. PGD_2 levels are significantly increased in bald scalp compared to haired scalp of patients with male pattern hair loss. Moreover, topically applied exogenous PGD_2 inhibits the hair growth of mice and explants of human hair follicles through the PGD_2-*GPR44* signaling pathway (Garza *et al.*, 2012). These results imply a regulatory network in hair follicles wherein PGD_2 inhibits, while $PGE_2/F_{2\alpha}$ promotes hair follicle function.

PGs are key inflammatory mediators involved in wound healing; however no study has examined their role in skin regeneration. We hypothesized that, given their presence during wound healing, PGs would impact wound-induced hair neogenesis (WIHN). With reports of PGE_2 promoting regeneration (Goessling *et al.*, 2009), we further hypothesized that PGD_2 would inhibit regeneration. In this study, we characterize the fluctuations of prostaglandins

throughout wound healing and demonstrate that levels of PGD_2 are inversely correlated with WIHN. Furthermore, we define an alternatively spliced transcript variant of lipocalin-type prostaglandin D_2 synthase (*Ptgds*, *L-pgds*) that correlates with the regeneration phenotype among several strains of mice. We demonstrate that PGD_2 inhibits hair follicle regeneration through the Gprotein coupled receptor *Gpr44* (DP-2).

Results

PGD_2 and PGE_2 are expressed in reciprocal patterns during wound healing

PG levels during incisional wounding in mice using enzyme immunoassays have been previously published (Kapoor *et al.*, 2007). In our study, we measured PGs during full-thickness excisional wounding in mice by mass spectrometry (Bell-Parikh *et al.*, 2003). In addition to the absolute PG levels, the expression of PG synthase enzymes was assessed by qRT-PCR.

Anesthetized adult C57Bl/6J mice were wounded with a $1cm^2$ full-thickness dorsal skin excision down to the level of skeletal muscle on post-natal day 21 (p21). The epidermis and dermis at the wound edge were sampled at various timepoints from pre-injury to 15 days postinjury. Histology revealed the emergence of an inflammatory infiltrate by post-wound day (PWD) 5. The healed wounds at PWD14 showed thickened epidermal and dermal layers compared to unwounded normal skin (Fig 1a). PGE_2 and $PGF_{2\alpha}$ levels increased early in wound healing while PGD_2 increased during the later stages of wound healing (PWD8 and onward) (absolute levels, Fig 1b; relative to baseline, 1c). Matching the relative levels of their products, mRNA levels of prostaglandin synthase enzyme for PGE_2 (*Ptges*) are significantly elevated during the early phases of wound healing while PGD_2 synthase (*Ptgds*) levels are elevated during the later stages of healing (Fig 1d).

PGD_2 levels inversely correlate with wound-induced hair neogenesis (WIHN)

To investigate whether PGD_2 inhibits hair follicle regeneration after wounding, we examined PGD_2 synthase and actual PGD_2 levels according to regeneration phenotype using three distinct background strains of mice: C57Bl/6J, FVB/N and Mixed (C57Bl/6J × FVB/N × SJL). Anesthetized adult mice (p21) were wounded with a $1cm^2$ full-thickness dorsal wound as above. The wound was allowed to heal by contraction and re-epithelialization, which was complete approximately 12 days after wounding. The resulting visible scar was $2–4mm^2$ in size. The numbers of regenerated hair follicles within the scar were detected by whole-mount keratin 17 immunohistochemistry on isolated epidermis between PWD 20–24. Hair follicles formed within a discrete area of the center of the scar (Fig 2a). Histology of K17-positive de novo hair follicles was confirmed with cross-sectional immunohistochemistry; adjacent sebaceous glands are also noted (Supp Fig 1).

Distinct levels of follicle regeneration were quantified among the different mouse strains, similar to published studies (Ito *et al.*, 2007). C57BL/6J mice had the least amount of follicle regeneration (~5 follicles) while the Mixed strain background had a mean of 20 follicles, a 4-fold increase in follicle regeneration (Fig 2b). Next, we examined PGD_2 synthase (*Ptgds*) levels among strains. Prior to the appearance of regenerated hair follicles at

PWD20, mRNA levels of *Ptgds* were measured on ~PWD12 in the re-epithelialized skin. *Ptgds* levels negatively correlate with regeneration when strain backgrounds are compared. C57Bl/6J mice had the highest level of *Ptgds* mRNA expression and the lowest amount of follicle neogenesis (Fig 2c). Conversely, the Mixed strain had the lowest *Ptgds* mRNA expression and the highest amount of follicle neogenesis. Levels of regeneration and *Ptgds* were both intermediate in FVB.

Next we measured the individual levels of PGD_2, PGE_2 and $PGF_{2\alpha}$ in re-epithelialized skin at PWD12 by mass spectrometry. The capacity to make PGD_2 corresponded to the degree of expression of *Ptgds* across the strains; PGD_2 levels were greatest within C57Bl/6J mice, intermediate within FVB/N and lowest in Mixed strain mice (Fig 2d). The levels of PGE_2 and $PGF_{2\alpha}$ did not display a similar pattern and the levels of $PGF_{2\alpha}$ in skin were 10-fold less than both PGD_2 and PGE_2 (Fig 2e, 2f). PGE_2 or $PGF_{2\alpha}$ did not correlate with regeneration ability across all strains. With no clear positive or negative correlation to the regeneration phenotype in the mouse strains, analysis was not continued for PGE_2 or $PGF_{2\alpha}$. These results demonstrated that the PGD_2 pathway, but not the PGE_2 or $PGF_{2\alpha}$, pathway correlates with the degree of wound-induced hair neogenesis; regeneration ability was inversely related to PGD_2 levels.

Ptgds splice variant missing exon 3 correlates with low regeneration

Given that *Ptgds* mRNA expression and its product PGD_2 negatively correlated with the observed follicle regeneration among the strains of mice, we focused our investigation on understanding the location and expression of *Ptgds*. We localized *Ptgds* mRNA and protein within re-epithelialized skin (PWD12) from C57Bl/6J mice. For detection of RNA, we enzymatically separated epidermis from dermis and quantified *Ptgds* mRNA levels by qRT-PCR on each fraction. *Ptgds* was more abundant in epidermis than dermis (Fig 3a). *Ptgds* was detected by immunohistochemistry predominantly in the scar epidermis, within the cytoplasm of keratinocytes, rather than dermis (Fig 3b). There is precedence for *Ptgds* expression within epithelial tissues of the retina and gastric mucosa as well as in keratinocytes of the skin (Black *et al.*, 2010; Garza *et al.*, 2012; Hokari *et al.*, 2009; Takeda *et al.*, 2006). Consistent with the sporadic expression of *Ptgds* we detected in the dermis, fibroblasts can express *Ptgds* during injury and serve as a source of PGD_2 (Hokari *et al.*, 2009).

Noting no discernable differences in the location of *Ptgds* protein between mouse strains and unable to detect changes in protein expression by immunoblotting, we investigated the possibility of alternative splicing of *Ptgds* as a possible explanation for lower levels of *Ptgds* mRNA and its resulting product, PGD_2. We investigated expression of *Ptgds* splice variants in re-epithelialized skin at PWD12 of C57Bl/6J, FVB/N and Mixed strain mice using Affymetrix exon probes followed by analysis with Partek Genome Studio software. We discovered that expression of exon 3 of the *Ptgds* gene varied significantly among our strains. Exon 3 expression was most abundant in C57Bl/6J and least expressed within Mixed strain mice. FVB/N mice demonstrated an intermediate level of exon 3 expression (Fig 3c). Thus, the expression of exon 3 was inversely correlated with the observed follicle regeneration in each strain (Fig 2a, 2b). Exons 1, 4 and 5 also had differential splicing

correlating to regeneration ability, but these differences were of much smaller magnitude; thus, we focused our further efforts on exon 3. These findings for exon 3 were confirmed with PCR using cDNA from PWD12 re-epithelialized skin in separate animals. PCR primers (Primer Set 1, Supp Fig 2) not in common with the Affymetrix probe were selected to border exon 3 (located within exon 2 and exon 4), thus detecting the presence or absence of exon 3 (Fig 3d). Two additional independent primer sets (Primer set 2 & 3; Supp Fig 2) were also used to validate these results. Sanger sequencing was performed on the PCR products (Primer Sets 1 and 2) and a portion of *Ptgds* exon 3 is absent as noted by analysis using BLAST software (Fig 3f). Furthermore, in Mixed strain mice, additional smaller bands were detected by PCR with Primer Set 3 (Supp Fig 3). DNA sequencing confirmed the absence of Exon 2; thus, we identified a second splice variant of *Ptgds*, (Supp Fig 3).

In summary, using Affymetrix probes followed by three independent sets of primers for traditional PCR with DNA sequencing, we corroborated our finding that C57Bl/6J mice have a higher proportion of non-spliced *Ptgds*, while our Mixed strain has a higher proportion of *Ptgds* missing exon 3 (Fig 3d, 3e, 3f). In summary, *Ptgds* is preferentially spliced in strains of mice with higher levels of follicle regeneration.

PGD_2 inhibits wound-induced hair follicle neogenesis through Gpr44

Finally, we directly investigated the effect of exogenous PGD_2 on regeneration. First, we investigated whether PGD_2 inhibits follicle neogenesis in wild type mice. Due to higher mean levels of follicle regeneration, Mixed strain mice were used for these experiments. After wounding, PGD_2 was topically applied to healing wounds, beginning at PWD7 through two days post scab detachment. *De novo* hair follicles were assessed as in Fig 2a. Exogenous PGD_2 decreased follicle regeneration in wild type mice compared to controls (Fig 4a).

More convincing evidence of PGD_2 inhibition of follicle regeneration was sought using knockout mouse models. PGD_2 activity is mediated via binding to two G protein coupled receptors: prostaglandin D_2 receptor (*Ptgdr, DP, DP-1*) and *Gpr44* (*Crth2; DP-2*) (Ricciotti and FitzGerald, 2011). The role of PGD_2 signaling was investigated using individual PGD_2 receptor knockout mice, $Ptgdr^{-/-}$ and $Gpr44^{-/-}$ as well as strain-matched (C57Bl/6J) control mice. Mice were wounded as above, with counting of *de novo* follicles on PWD20 as a measure of regenerative capacity. qRT-PCR determined that each of the two receptors was expressed at similar levels in wild type mice in normal skin as well as within healed scars. Previous studies demonstrated *Ptgdr* and *Gpr44* expression within epidermal and follicular keratinocytes (Colombe *et al.*, 2008). Mice lacking *Ptgdr* or *Gpr44* receptors are phenotypically normal, with no observed skin, hair follicle or hair cycling defects. There was no difference in follicle regeneration after wounding between control mice and $Ptgdr^{-/-}$ mice. However, in mice lacking *Gpr44*, follicle regeneration was significantly increased (~2-fold) compared to wild type and $Ptgdr^{--/-}$ mice; mice that were heterozygous for *Gpr44* had an intermediate level of regenerated follicles, but were not significantly different from wild type or knockout mice (Fig 4b).

We further examined the impact of PGD_2 on mice that are heterozygous or null for *Gpr44*. Using additional cohorts of heterozygous and $Gpr44^{-/-}$ mice, we evaluated the effect of

PGD_2 on WIHN. PGD_2 was topically applied to healing wounds, beginning at PWD7 through two days post scab detachment. Exogenous PGD_2 did not significantly affect follicle regeneration in *Gpr44*$^{+/-}$ or *Gpr44*$^{-/-}$ mice compared to vehicle control (Fig 4c). As before, follicle regeneration with vehicle control was increased in null mice when compared to *Gpr44*$^{+/-}$ mice, although not significantly.

The application vehicle for PGD_2 used in Figure 4c influenced follicle regeneration; vehicle increased the number of regenerated follicles in scars by an average of 9 follicles compared to non-vehicle treated mice ($n>10$; $p< 0.05$) for *Gpr44* null mice. Therefore, comparisons cannot be made between figure panels b and c. Also, results in Figure 4a cannot be compared to Figure 4b or 4c due to inherent variation in the strains.

Together, the ability of exogenous PGD_2 to inhibit WIHN in wild type mice, the increased level of WIHN in *Gpr44* null mice, and the resistance to PGD_2 inhibition of WIHN in *Gpr44*$^{-/-}$ mice, collectively demonstrate that the mechanism for PGD_2 inhibition of WIHN occurs through *Gpr44* activation.

Discussion

Wound healing usually results in inadequate tissue repair by scarring or fibrosis. In some cases, however, tissue regeneration can occur. Our understanding of the control of wound scarring versus tissue regeneration is incomplete. The contribution of inflammatory mediators, including prostaglandins, during the wound healing process is well-established. PG functions during tissue regeneration are less studied, but it is known that PGE_2 can stimulate liver regeneration (Goessling *et al.*, 2009). Given the demonstration of increased hair growth by $PGF_{2\alpha}$ and PGE_2 (Geng *et al.*, 1992; Sasaki *et al.*, 2005) as well as decreased hair growth by PGD_2 (Garza *et al.*, 2012), we hypothesized that these prostaglandins may be important in regulating hair neogenesis in WIHN. Normal hair growth is regulated by transition between catagen, anagen and telogen phases of the hair cycle. During anagen, the hair follicle partially regenerates, suggesting that pathways which control the hair regeneration cycle may also control hair follicle neogenesis. In this manuscript, we demonstrated that PGD_2 correlates with decreased follicle regeneration after wounding, that PGD_2 has the capacity to inhibit follicle regeneration and that the mechanism of this inhibition is through the *Gpr44* receptor.

One previously unreported discovery is that *Ptgds* is alternatively spliced, such that partial removal of exon 3 correlates with higher levels of regeneration. The absence of exon 3 likely affects the functionality of the final product. The structure of *Ptgds* is that of the typical lipocalin β-barrel comprised of eight anti-parallel β-barrel strands, three α helical regions and a C-terminal β-strand. *Ptgds* is the only enzyme within the lipocalin family of proteins; it catalyzes the formation of PGD_2 from PGH_2. Like other lipocalin family members, Ptgds also functions as a transport protein for lipophilic compounds like retinoids, gangliosides, bilirubin and β-amyloid peptides (Akerstrom *et al.*, 2000). Exon 3 of *Ptgds* encodes amino acids 86 through 110 of the protein sequence, forming the D and E strands (Shimamoto *et al.*, 2007). The E strand, together with the F strand, forms the flexible E-F loop responsible for the open/closed formations of the calyx. Based on our sequence results,

20 amino acids are removed from exon 3, including Leu96 and Cys89. Leu96 in exon 3, with its bulky side chain, along with other nearby hydrophobic amino acids, acts to divide the central cavity into two compartments: one for binding and converting PGH_2 to PGD_2, while the other compartment binds lipophilic compounds, such as retinoids (Kumasaka *et al.*, 2009). Cys89 in exon 3 forms a disulfide bridge with Cys186, which is important in stabilizing the protein structure. In all, exon 3 encodes amino acids involved in central cavity division, open/closed conformation formation and protein stability.

We also identified a splice variant of *Ptgds* that completely lacks exon 2 (Supp Fig 3). Four key serine, theronine and cysteine moieties are located within exon 2 and mutations within these residues dramatically decrease *Ptgds* enzymatic activity (Shimamoto *et al.*, 2007). Alternative splicing of *Ptgds*, such that portions of exon 2 or exon 3 are absent may result in decreased functionality of *Ptgds* and contribute to the lower level of PGD_2 found in the strains expressing spliced Ptgds. In support of this hypothesis, an alternative splice variant of cyclooxygenase 1 (Cox-1) lacking 37 amino acids in exon 9, results in no detectable PGH_2 product (Schneider *et al.*, 2005). Conversely, splice variants of receptor and enzymes can exert dominant negative effects over their complete signaling and catalytically active forms (Stamm *et al.*, 2005).

We also found that during wound healing, the capacity of tissue to generate PGE_2 and PGD_2 is separated over time, thus providing evidence consistent with the distinct functions of prostaglandins. These results are similar to those observed after incisional wound healing in DBA/I mice (Kapoor *et al.*, 2007). In C57Bl/6J and DBA/I strains and models of wound healing, PGE_2 is the more abundant product during the early phases of wound healing. Elevated levels of PGE_2, a potent immune activator, are consistent with progressing inflammation (Sakata *et al.*). Whereas, at later stages when inflammation is resolving, PGE_2 levels taper off and PGD_2 becomes the predominant prostaglandin.

Our final previously unreported finding was that the mechanism of PGD_2 inhibition of wound-induced hair neogenesis is through the *Gpr44* receptor. *Gpr44* is expressed on immune cells including eosinophils, neutrophils, mast cells, basophils, a subpopulation of memory Th_2 cells and monocytes (Nagata *et al.*, 1999a; Nagata *et al.*, 1999b). It mediates the chemotaxis of these pro-inflammatory cells during allergic inflammation (Hirai *et al.*, 2001). Our results show that in the absence of *Gpr44*, WIHN is increased in our experimental wound model, which suggests that follicle regeneration is possible in the absence of this pro-inflammatory milieu of cells. Likewise, WIHN is suppressed in wild type mice in the presence of PGD_2, arguing that the presence of pro-inflammatory mediators inhibits regeneration.

While these data suggest that *Gpr44* normally inhibits WIHN through recruitment of inflammatory cells, alternative interpretations are possible. *Gpr44* null mice show features of both enhanced and decreased airway inflammation (Chevalier *et al.*, 2005; Shiraishi *et al.*, 2008). Conflicting data in the literature demonstrates that PGD_2 both enhances and reduces allergic responses, with the *Gpr44* receptor playing a critical role (Arimura *et al.*, 2001; Hammad *et al.*, 2007; Matsuoka *et al.*, 2000; Matsushima *et al.*, ; Satoh *et al.*, 2006;

Shiraishi *et al.*, 2008; Trivedi *et al.*, 2006; Yamamoto *et al.*). It is therefore also possible that PGD_2's actions through *Gpr44* may inhibit pro-regenerative immune factors.

A motivation for this study is the ability of PGD_2 to inhibit hair lengthening (Garza *et al.*, 2012). Here we demonstrate that PGD_2 also inhibits hair regeneration after wounding. Thus, PGD_2 and *Gpr44* inhibition of the hair follicle occurs in multiple contexts and may be exploited in future therapies. Pharmaceutical companies are already focused on the development of *Gpr44*- selective antagonists for the treatment of asthma with at least nine other known *Gpr44* antagonists in Phase II clinical trials (Jones *et al.*, 2009; Norman, 2010; Pettipher and Whittaker). In addition to previous studies suggesting that *Gpr44* antagonists may be beneficial in androgenetic alopecia, our results suggest that formulations of *Gpr44* antagonists may decrease scarring during wound healing. A specific example is ramatroban, an orally-active, dual *Gpr44* and thromboxane A2 receptor antagonist, which is approved in Japan for the treatment of allergic rhinitis in humans (Sugimoto *et al.*, 2003). Future studies could examine the effect of ramatroban in stimulating hair follicle neogenesis.

Materials and Methods

Animals

All animal protocols are approved by the Johns Hopkins University Animal Care and Use Committee. C57Bl/6J, FVB/N and Mixed strain (C57Bl/6J × FVB/N × SJL/J) animals were obtained from The Jackson Laboratory and George Cotsarelis (UPENN). $Ptgdr^{-/-}$, $Gpr44^{-/-}$ $Ptgds^{-/-}$ knockout mice were obtained from original sources as previously described (Garza et al, 2012). Heterozygous mice for *Gpr44* were bred by crossing WT and $Gpr44^{-/-}$ animals; genotype was verified by PCR with the following primers: 5'-CTC-GCC-GGA-CAC-GCT-GAACTT- GT-3', 5'-TGG-GGT-CAA-ACT-CAG-CTC-CTC-ACG-3' and 5'-GCG-GCG-GCT-AACAAG- TCG-GAT-AG -3'. All animal colonies were maintained within animal facilities with standard humidity, 12 hour light/dark cycle and laboratory diet *ad libitum*. Both male and female mice were used in our experiments and gender did not impact our results.

Wound Induced Hair Neogenesis (WIHN) Assay

A 1 cm^2 full-thickness wound on the backs of 21-day old male and female mice was performed as previously described (Ito *et al.*, 2007). Scars were harvested 8–12 days after the scab detached from the wound (PWD20-24). This time point represents approximately 16 days after contraction has ended and approximately 14 days after re-epithelialization has occurred. The dermis and epidermis were separated using overnight EDTA treatment and stained for keratin 17 (Abcam Inc, Cambridge MA) on whole mount epidermis to identify regenerated hair follicles. Numbers of regenerated follicles were quantified in the re-epithelialized skin as published (Ito *et al.*, 2007).

Mass Spectrometry

Baseline tissue, a 1-cm^2 piece of full-thickness skin, was taken from each animal at wounding. Wound edges from 1 hour, 1 day, 3 days and 5 days post-wounding and re-epithelialized tissue (healed scar) at PWD12, PWD14 and PWD16 were collected for

analysis. All samples were collected in acetone, frozen in liquid nitrogen and stored at −80°C. Prostaglandins were isolated from samples by tissue homogenization in acetone for 90 seconds. Samples were centrifuged at 13,500 rpm at 4°C for 10 minutes and the resulting supernatant was assessed for PGD_2, PGE_2 and $PGF_{2\alpha}$ levels by mass spectrometry as described (Garza *et al.*, 2012).

Quantitative real-time PCR (qRT-PCR)

The levels of gene expression were accessed by qRT-PCR in a parallel time course to that of mass spectrometry. For mRNA analysis, samples were collected and stored in *RNA Later*© (Sigma, St Louis MO) at −20°C. Early time points contained wound-edge only (~1–2mm border) and time points after re-epithelialization consisted of the "scar area" only. Samples were homogenized using a tissue grinder, processed with RNeasy Fibrous Tissue kit (Qiagen, Valencia, CA) and transcribed to cDNA (High Capacity RNA to cDNA; Applied Biosystems, Carlsbad, CA). qRT-PCR was performed on samples (50ng cDNA) for genes of interest using inventoried TaqMan gene expression assays from Applied Biosystems. Differences in gene expression were assessed by comparative $\Delta\Delta C_T$ values with fold change calculations.

Immunohistochemistry

Immunohistochemistry was performed on formalin-fixed paraffin-embedded mouse skin sections using the avidin-biotin complex method and AEC development (ABC kit and AEC Substrate kit for Peroxidase; Vector Laboratories). Baseline and ~PWD12 healed scars were subjected to deparaffinization, rehydration and antigen retrieval with TRILOGY buffer (Cell Marque) prior to immunohistochemistry. Sections were incubated overnight with rabbit polyclonal Ptgds antibody (LifeSpan Biosciences Inc. Seattle, WA). For Supplemental Figure 1, Cytokeratin 17 (Abcam, Cambridge, MA) was used. Negative controls were prepared with purified rabbit IgG antibody (Invitrogen, Camarillo, CA). Sections were counterstained with hematoxylin using standard procedures.

Ptgds splice variant analysis

Splice variant analysis among mouse strains within *Ptgds* gene were identified and analyzed by Partek Genome Studio software (Partek INC., Saint Louis MO, USA). Splice variant expression within the third exon was confirmed by standard PCR and agarose gel electrophoresis. Primers are as follows: sense 5' AGGGCCATGACACAGTGCAGC and antisense 3' GAGGGTGGCCATGCGGAAGTC (Primer Set 1) which identifies a 371 base pair amplicon for the complete exon 3 compared to a 300 base pair amplicon if exon 3 is affected. These initial PCR results were confirmed by two additional primer sets: Primer Set 2 with amplicons 371 and 300 respectively, 5' AGGGCCATGACACAGTGCAGCCCAACTTTC and 3' GAGGGTGGCCATGCGGAAGTCCTGGCCTGGG; and Primer Set 3-5' AAGACAAGTTCCTGGGGCGCTG and 3'-GTGGATGCTGCCCGAGTGGG (amplicons of ~240 versus ~180 with exon 3 splicing). See Supplemental Figure 3 for all primer locations. cDNA was subjected to PCR with PCR MasterMix (Promega, Madison WI) and

Veriti Thermal Cycler (Applied Biosystems INC, Carlsbad CA). Relative quantification of PCR results was assessed by Image J software.

Topical PGD_2 treatment

PGD_2 (Cayman Chemical, Ann Arbor, MI), was reconstituted in ethanol at a concentration of 50mg/mL. 10μg PGD_2 in ethanol/5% polyethylene glycol/2% glycerol was applied daily beginning on PWD7 and continued daily until two days post scab detachment. Ethanol/polyethylene glycol/glycerol alone was applied in parallel for vehicle control. Regenerated hair follicles were assessed by K17 IHC at PWD20-24.

Statistical Analysis

Each experiment was repeated with at least 3 independent litters of animals. Numbers of independent animals are noted for each experiment. Data was analyzed using paired *t*-test or ANOVA single factor. Statistical significance was considered at $p < 0.05$.

Supplementary Material

Refer to Web version on PubMed Central for supplementary material.

Acknowledgements

The authors thank Sydney Resnik and Shalini Maitra for critical reading of this manuscript and C. C. Talbot Jr., for technical assistance. We acknowledge Drs. George Cotsarelis and Mayumi Ito for helpful advice. Dr. FitzGerald is the Robert McNeill Professor of Translational Medicine and Therapeutics. This work was supported by grants from the Dermatology Foundation, NIH (NIAMS K08 AR055666) to LAG and the Department of Dermatology, Johns Hopkins School of Medicine.

References

Akerstrom B, Flower DR, Salier J-P. Lipocalins: unity in diversity. Biochimica et Biophysica Acta (BBA) - Protein Structure and Molecular Enzymology. 2000; 1482:1–8. [PubMed: 11058742]

Arimura A, Yasui K, Kishino J, Asanuma F, Hasegawa H, Kakudo S, et al. Prevention of allergic inflammation by a novel prostaglandin receptor antagonist, S-5751. J Pharmacol Exp Ther. 2001; 298:411–419. [PubMed: 11454901]

Bell-Parikh LC, Ide T, Lawson JA, McNamara P, Reilly M, FitzGerald GA. Biosynthesis of 15-deoxy-delta12,14-PGJ2 and the ligation of PPARgamma. J Clin Invest. 2003; 112:945–955. [PubMed: 12975479]

Black AT, Joseph LB, Casillas RP, Heck DE, Gerecke DR, Sinko PJ, et al. Role of MAP kinases in regulating expression of antioxidants and inflammatory mediators in mouse keratinocytes following exposure to the half mustard, 2-chloroethyl ethyl sulfide. Toxicology and Applied Pharmacology. 2010; 245:352–360. [PubMed: 20382172]

Bol DK, Rowley RB, Ho CP, Pilz B, Dell J, Swerdel M, et al. Cyclooxygenase-2 overexpression in the skin of transgenic mice results in suppression of tumor development. Cancer Res. 2002; 62:2516–2521. [PubMed: 11980643]

Chevalier E, Stock J, Fisher T, Dupont M, Fric M, Fargeau H, et al. Cutting edge: chemoattractant receptor-homologous molecule expressed on Th2 cells plays a restricting role on IL-5 production and eosinophil recruitment. J Immunol. 2005; 175:2056–2060. [PubMed: 16081770]

Colombe L, Michelet JF, Bernard BA. Prostanoid receptors in anagen human hair follicles. Exp Dermatol. 2008; 17:63–72. [PubMed: 18005048]

Colombe L, Vindrios A, Michelet JF, Bernard BA. Prostaglandin metabolism in human hair follicle. Exp Dermatol. 2007; 16:762–769. [PubMed: 17697149]

Garza LA, Liu Y, Yang Z, Alagesan B, Lawson JA, Norberg SM, et al. Prostaglandin D2 Inhibits Hair Growth and Is Elevated in Bald Scalp of Men with Androgenetic Alopecia. Science Translational Medicine. 2012 in revised submission.

Geng L, Hanson WR, Malkinson FD. Topical or systemic 16, 16 dm prostaglandin E2 or WR-2721 (WR-1065) protects mice from alopecia after fractionated irradiation. Int J Radiat Biol. 1992; 61:533–537. [PubMed: 1349335]

Goessling W, North TE, Loewer S, Lord AM, Lee S, Stoick-Cooper CL, et al. Genetic Interaction of PGE2 and Wnt Signaling Regulates Developmental Specification of Stem Cells and Regeneration. Cell. 2009; 136:1136–1147. [PubMed: 19303855]

Hammad H, Kool M, Soullie T, Narumiya S, Trottein F, Hoogsteden HC, et al. Activation of the D prostanoid 1 receptor suppresses asthma by modulation of lung dendritic cell function and induction of regulatory T cells. J Exp Med. 2007; 204:357–367. [PubMed: 17283205]

Han M, Yang X, Taylor G, Burdsal CA, Anderson RA, Muneoka K. Limb regeneration in higher vertebrates: developing a roadmap. Anat Rec B New Anat. 2005; 287:14–24. [PubMed: 16308860]

Hirai H, Tanaka K, Yoshie O, Ogawa K, Kenmotsu K, Takamori Y, et al. Prostaglandin D2 selectively induces chemotaxis in T helper type 2 cells, eosinophils, and basophils via seven-transmembrane receptor CRTH2. J Exp Med. 2001; 193:255–261. [PubMed: 11208866]

Hokari R, Nagata N, Kurihara C, Watanabe C, Komoto S, Okada Y, et al. Increased expression and cellular localization of lipocalin-type prostaglandin D synthase in Helicobacter pylori-induced gastritis. The Journal of Pathology. 2009; 219:417–426. [PubMed: 19768745]

Ito M, Yang Z, Andl T, Cui C, Kim N, Millar SE, et al. Wnt-dependent de novo hair follicle regeneration in adult mouse skin after wounding. Nature. 2007; 447:316–320. [PubMed: 17507982]

Jia C. Advances in the regulation of liver regeneration. Expert Rev Gastroenterol Hepatol. 2011; 5:105–121. [PubMed: 21309676]

Johnstone MA, Albert DM. Prostaglandin-induced hair growth. Surv Ophthalmol. 2002; 47(Suppl 1):S185–S202. [PubMed: 12204716]

Jones RL, Giembycz MA, Woodward DF. Prostanoid receptor antagonists: development strategies and therapeutic applications. Br J Pharmacol. 2009; 158:104–145. [PubMed: 19624532]

Kapoor M, Kojima F, Yang L, Crofford LJ. Sequential induction of pro- and anti-inflammatory prostaglandins and peroxisome proliferators-activated receptor-gamma during normal wound healing: a time course study. Prostaglandins Leukot Essent Fatty Acids. 2007; 76:103–112. [PubMed: 17239574]

Kumasaka T, Aritake K, Ago H, Irikura D, Tsurumura T, Yamamoto M, et al. Structural basis of the catalytic mechanism operating in open-closed conformers of lipocalin type prostaglandin D synthase. J Biol Chem. 2009; 284:22344–22352. [PubMed: 19546224]

LS Goodman, AG.; Hardman, JG.; Gilman, AG.; Limbird, LE. Goodman & Gilman's the pharmacological basis of therapeutics. 9th edn.. New York: McGraw-Hill, Health Professions Division; 1996. p. xxi1905 p., [1] p. folded plate.

Matsuoka T, Hirata M, Tanaka H, Takahashi Y, Murata T, Kabashima K, et al. Prostaglandin D2 as a mediator of allergic asthma. Science. 2000; 287:2013–2017. [PubMed: 10720327]

Matsushima Y, Satoh T, Yamamoto Y, Nakamura M, Yokozeki H. Distinct roles of prostaglandin D2 receptors in chronic skin inflammation. Mol Immunol. 2011; 49:304–310. [PubMed: 21943706]

Metcalfe AD, Willis H, Beare A, Ferguson MW. Characterizing regeneration in the vertebrate ear. J Anat. 2006; 209:439–446. [PubMed: 17005017]

Muller-Decker K, Scholz K, Neufang G, Marks F, Furstenberger G. Localization of prostaglandin-H synthase-1 and-2 in mouse skin: implications for cutaneous function. Exp Cell Res. 1998; 242:84–91. [PubMed: 9665805]

Nagata K, Hirai H, Tanaka K, Ogawa K, Aso T, Sugamura K, et al. CRTH2, an orphan receptor of T-helper-2-cells, is expressed on basophils and eosinophils and responds to mast cell-derived factor(s). FEBS Lett. 1999a; 459:195–199. [PubMed: 10518017]

Nagata K, Tanaka K, Ogawa K, Kemmotsu K, Imai T, Yoshie O, et al. Selective expression of a novel surface molecule by human Th2 cells in vivo. J Immunol. 1999b; 162:1278–1286. [PubMed: 9973380]

Neufang G, Furstenberger G, Heidt M, Marks F, Muller-Decker K. Abnormal differentiation of epidermis in transgenic mice constitutively expressing cyclooxygenase-2 in skin. Proc Natl Acad Sci U S A. 2001; 98:7629–7634. [PubMed: 11381142]

Norman P. DP2 receptor antagonists in development. Expert Opin Investig Drugs. 2010; 19:947–961.

Pettipher R, Whittaker M. Update on the development of antagonists of chemoattractant receptor-homologous molecule expressed on Th2 cells (CRTH2). From lead optimization to clinical proof-of-concept in asthma and allergic rhinitis. Journal of Medicinal Chemistry.

Price J, Faucheux C, Allen S. Deer antlers as a model of Mammalian regeneration. Curr Top Dev Biol. 2005; 67:1–48. [PubMed: 15949530]

Ricciotti E, FitzGerald GA. Prostaglandins and inflammation. Arterioscler Thromb Vasc Biol. 2011; 31:986–1000. [PubMed: 21508345]

Sakata D, Yao C, Narumiya S. Prostaglandin E2, an Immunoactivator. Journal of Pharmacological Sciences. 2010; 112:1–5. [PubMed: 20051652]

Sasaki S, Hozumi Y, Kondo S. Influence of prostaglandin F2alpha and its analogues on hair regrowth and follicular melanogenesis in a murine model. Exp Dermatol. 2005; 14:323–328. [PubMed: 15854125]

Satoh T, Moroi R, Aritake K, Urade Y, Kanai Y, Sumi K, et al. Prostaglandin D2 plays an essential role in chronic allergic inflammation of the skin via CRTH2 receptor. J Immunol. 2006; 177:2621–2629. [PubMed: 16888024]

Schneider C, Boeglin WE, Brash AR. Human cyclo-oxygenase-1 and an alternative splice variant: contrasts in expression of mRNA, protein and catalytic activities. Biochem J. 2005; 385:57–64. [PubMed: 15361066]

Shimamoto S, Yoshida T, Inui T, Gohda K, Kobayashi Y, Fujimori K, et al. NMR solution structure of lipocalin-type prostaglandin D synthase: evidence for partial overlapping of catalytic pocket and retinoic acid-binding pocket within the central cavity. J Biol Chem. 2007; 282:31373–31379. [PubMed: 17715133]

Shiraishi Y, Asano K, Niimi K, Fukunaga K, Wakaki M, Kagyo J, et al. Cyclooxygenase-2/prostaglandin D2/CRTH2 pathway mediates double-stranded RNA-induced enhancement of allergic airway inflammation. J Immunol. 2008; 180:541–549. [PubMed: 18097056]

Stamm S, Ben-Ari S, Rafalska I, Tang Y, Zhang Z, Toiber D, et al. Function of alternative splicing. Gene. 2005; 344:1–20. [PubMed: 15656968]

Sugimoto H, Shichijo M, Iino T, Manabe Y, Watanabe A, Shimazaki M, et al. An orally bioavailable small molecule antagonist of CRTH2, ramatroban (BAY u3405), inhibits prostaglandin D2-induced eosinophil migration in vitro. J Pharmacol Exp Ther. 2003; 305:347–352. [PubMed: 12649388]

Takeda K, Yokoyama S, Aburatani H, Masuda T, Han F, Yoshizawa M, et al. Lipocalintype prostaglandin D synthase as a melanocyte marker regulated by MITF. Biochemical and Biophysical Research Communications. 2006; 339:1098–1106. [PubMed: 16337607]

Trivedi SG, Newson J, Rajakariar R, Jacques TS, Hannon R, Kanaoka Y, et al. Essential role for hematopoietic prostaglandin D2 synthase in the control of delayed type hypersensitivity. Proc Natl Acad Sci U S A. 2006; 103:5179–5184. [PubMed: 16547141]

Yamamoto Y, Otani S, Hirai H, Nagata K, Aritake K, Urade Y, et al. Dual functions of prostaglandin D2 in murine contact hypersensitivity via DP and CRTH2. Am J Pathol. 179:302–314. [PubMed: 21703412]

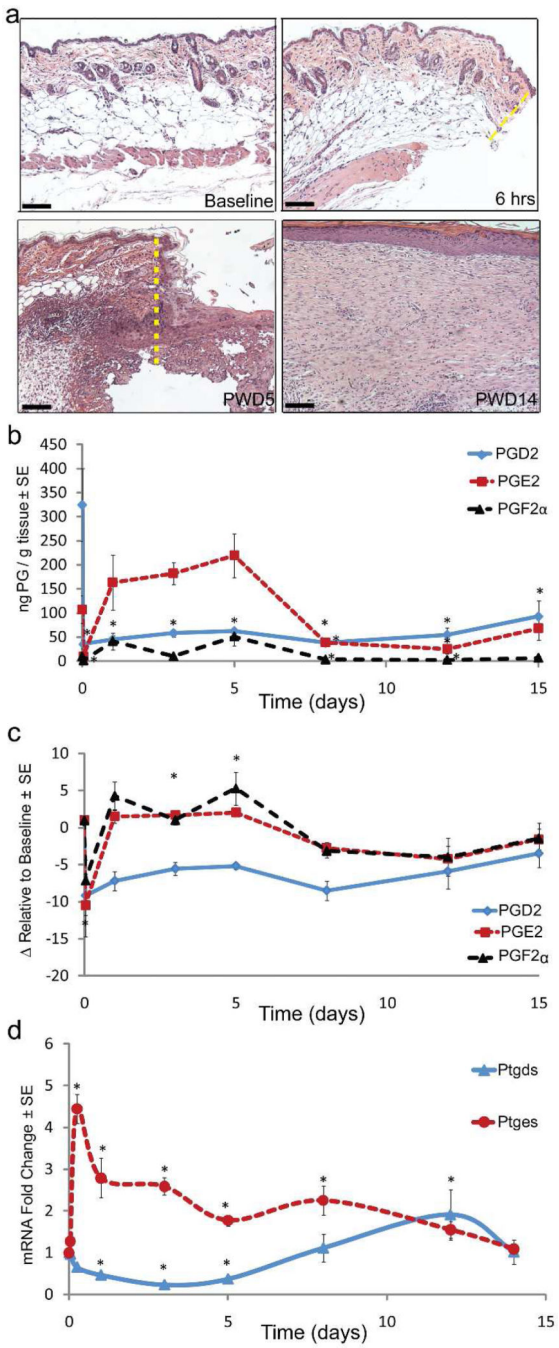

Figure 1. PGD_2 and PGE_2 are expressed in reciprocal patterns during wound healing

(a–e) Full excision skin wounding to the depth of skeletal muscle was performed on C57Bl/6J mice. On the listed days, tissue from the wound edge was sampled for measurement **(a)** Hematoxylin and eosin histology of normal (baseline), 6-hour wound edge, PWD5 and 2 days after scab detached (PWD14); wound edges shown with dashed line (yellow). Scale bar = 100μm **(b–c)** Levels of PGD_2, PGE_2 and $PGF_{2\alpha}$ measured by mass spectrometry, depicted in either **(b)** absolute ng/g tissue or as **(c)** fold change in ng/g tissue

relative to baseline; n = 3; $p < 0.05$. **(d)** mRNA expression of Ptgds1 and Ptges1 as determined by qRT-PCR. n = 3; $p < 0.05$.

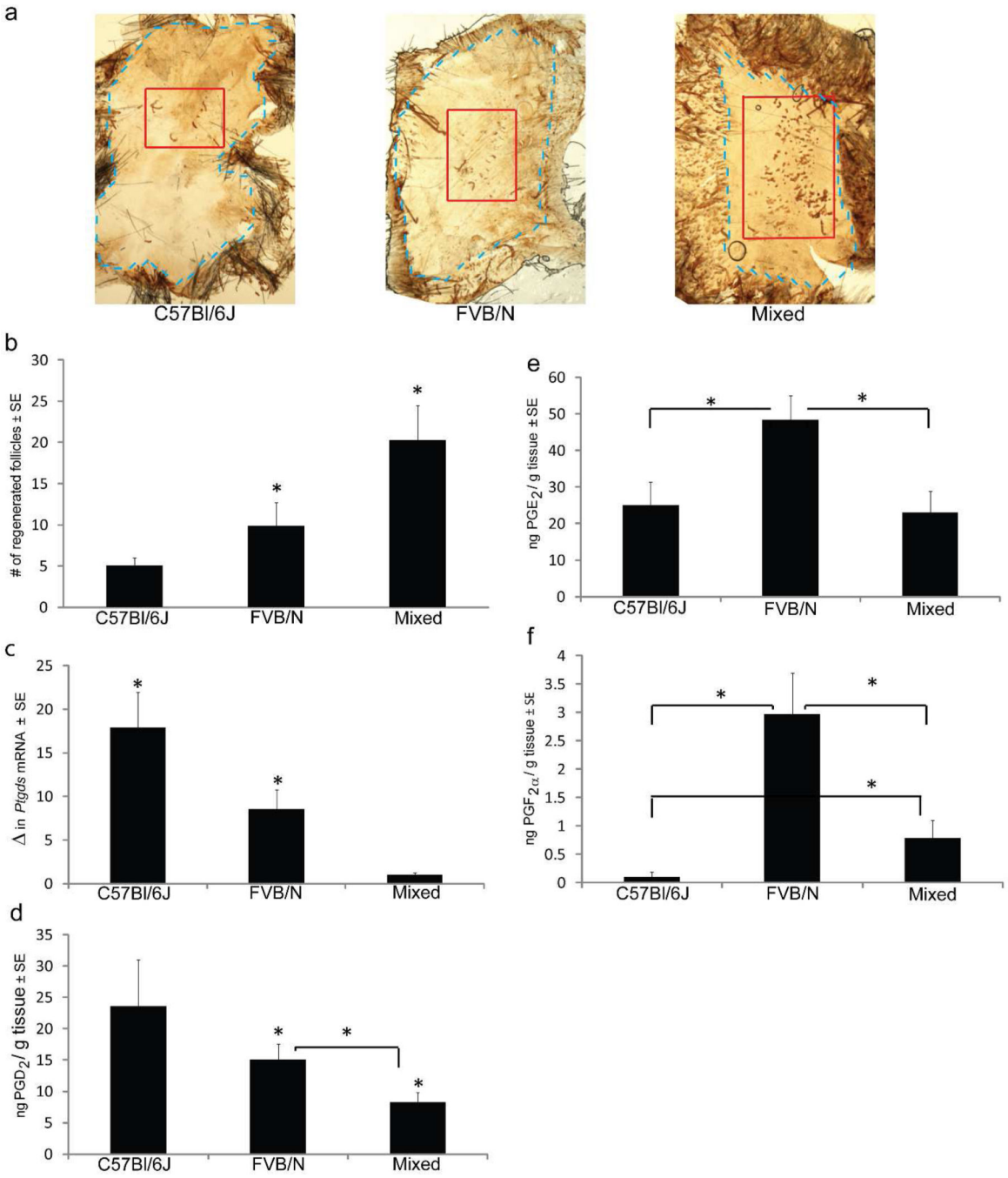

Figure 2. Prostaglandin D_2 levels negatively correlate with hair follicle regeneration

(a–e) Full excision skin wounding as described in Fig 1. was performed on C57Bl/6J, FVB/N and Mixed strain mice. **(a)** Hair follicle regeneration was assessed by K17 immunohistochemistry on isolated epidermis at PWD 20–24. Representative images are shown: scar outlined in blue, WIHN area within red. Scale bar: 100μm. **(b)** Quantification of regenerated follicles within scars by strain; $n \geq 33$, $p < 0.05$. **(c)** qRT-PCR of *Ptgds* mRNA levels (shown as fold change) in PWD12 re-epithelialized skin; $n = 3$, $p < 0.05$. **(d–f)** Mass

spectrometry measurement of individual prostaglandins in re-epithelialized skin at PWD12. **(d)** PGD_2; **(e)** $PGE_{2;\ and}$ **(f)** PGF_{2a}; $n > 3$; $p \leq 0.05$.

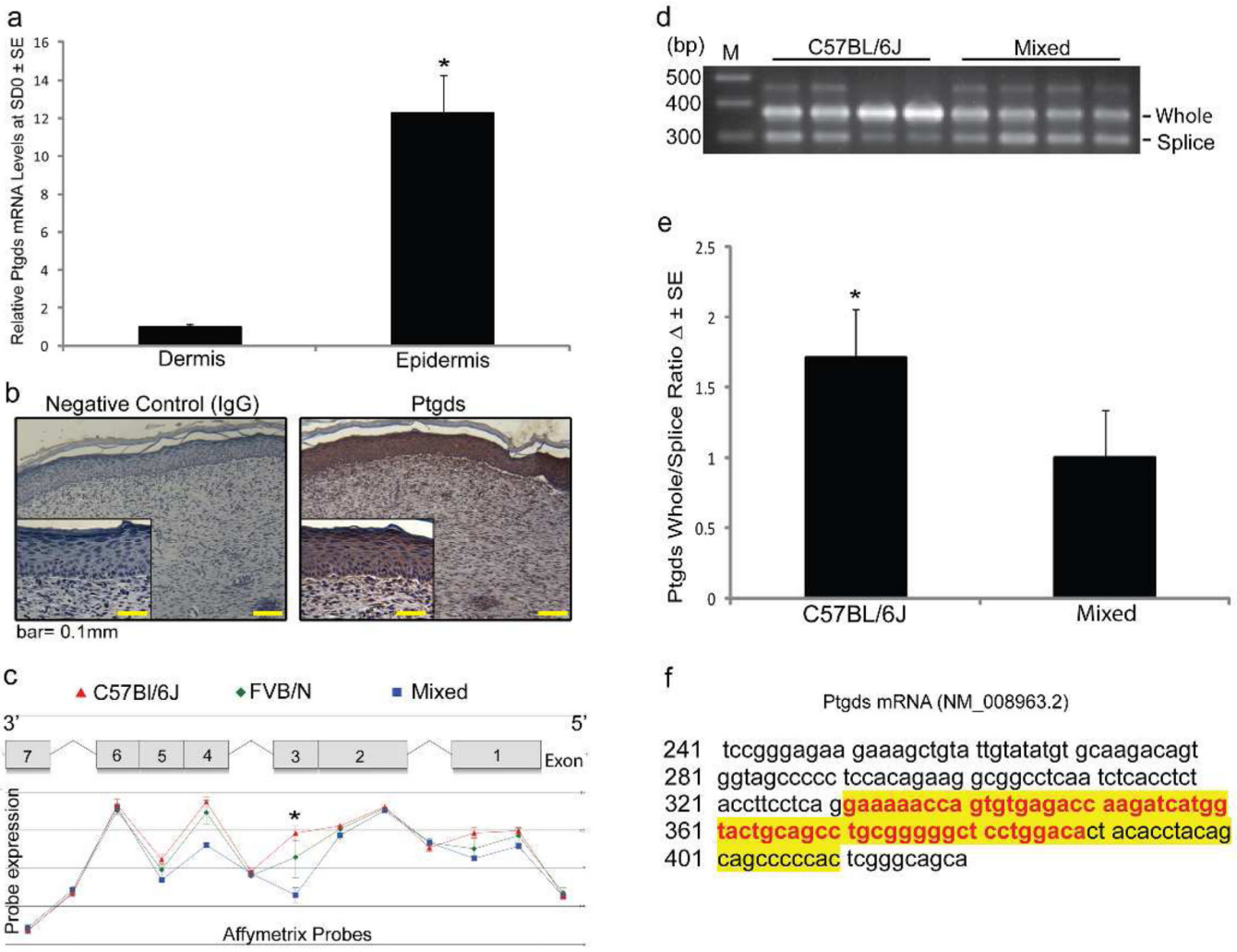

Figure 3. Splicing of Exon 3 in Ptgds positively correlates with hair follicle regeneration

(a–e) Newly re-epithelialized skin (~PWD12) after WIHN was excised then examined with qRT-PCR and immunohistochemistry. **(a)** C57Bl/6 skin was enzymatically separated into epidermis and dermis for qRT-PCR of Ptgds mRNA, n = 5–6 samples; $p < 0.05$. **(b)** Immunohistochemistry on C57Bl/6 skin with Ptgds polyclonal rabbit antibody and isotype control antibody. Total magnification is 100X with insets at 200X. Scale bar = 100μm. **(c)** mRNA isolated from the C57Bl/6J (red), FVB/N (green) and Mixed (blue) background strains was measured by Affymetrix® exon probes. *Ptgds* exon map with relative abundance levels of each exon graphed below according to strain, **(d)** PCR verification of *Ptgds* splice variant expression in C57Bl/6 and Mixed strains. PCR Primer Set 1 generates amplicon size of 371bp in the presence of exon 3 and 300bp with splicing of exon 3, and are independent probes from those used in **(c)**. Representative gel showing 4 samples of each strain shown. **(e)** Relative quantification of splice variant expression in mouse strains. A ratio of "whole exon 3" to "spliced exon 3" was used for analysis; n=9, $p < 0.05$. **(f)** Sanger sequencing of the PCR products (Primer Sets 1 and 2) confirms alternative splicing of *Ptgds* exon 3 (yellow highlight) with the missing portion of exon 3 in red.

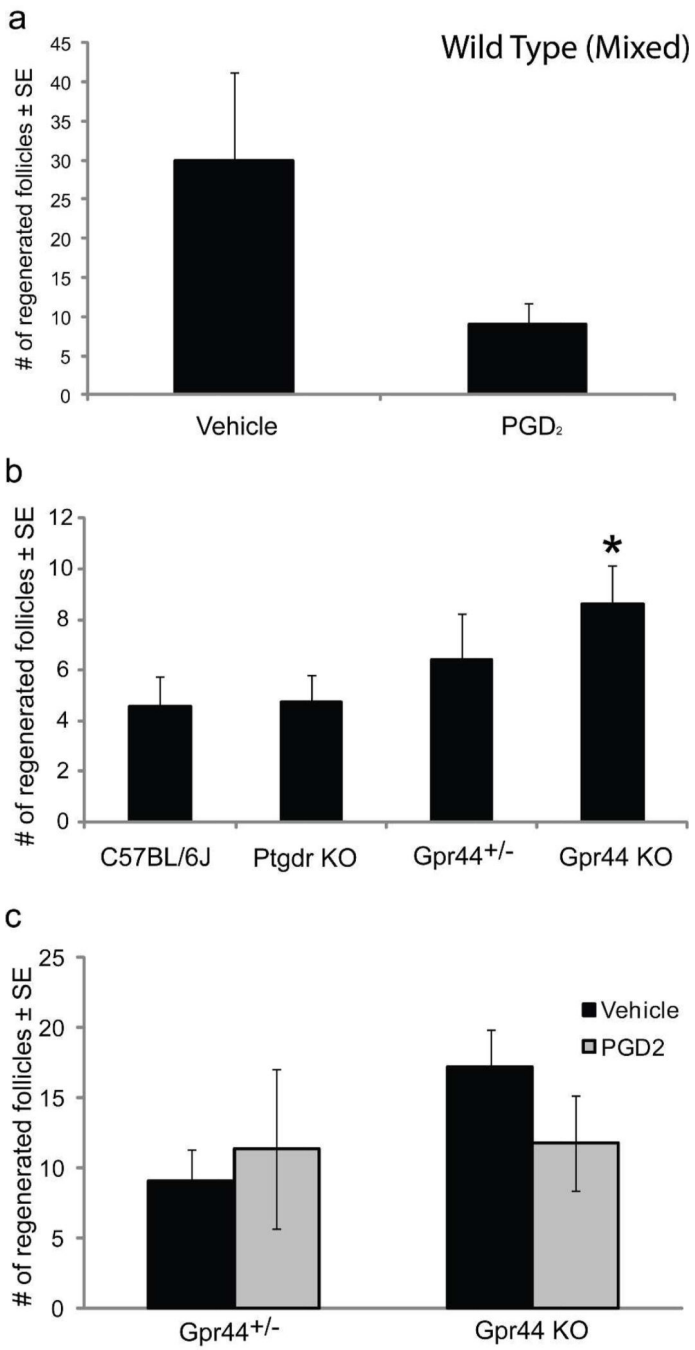

Figure 4. PGD_2 inhibits WIHN in wild type mice but not in *Gpr44* null mice, which otherwise have increased hair follicle regeneration

(a) Full excision wounding as described in Fig 1. was performed on Mixed strain mice with topical application of PGD_2 beginning on PWD7. Topical application of PGD_2 to wild type mice decreased WIHN; n = 7–9, p = 0.06. **(b)** Individual prostaglandin receptor null (*Ptgdr* KO and *Gpr44* KO), $Gpr44^{+/-}$ and WT (C57BL/6J) mice were subjected to the WIHN assay and regenerated follicles were detected by K17 immunohistochemistry. *Gpr44* KO mice had a 2-fold increase in regenerated follicles compared to wild type and Ptgdr KO mice; n = 21–

31 mice/genotype, $p < 0.05$. *Gpr44*$^{+/-}$ mice demonstrated an intermediate level of regeneration. **(c)** WIHN assay was performed on *Gpr44*$^{+/-}$ and *Gpr44* KO mice with topical application of PGD_2 beginning at PWD7. Topical application of PGD_2 to both *Gpr44*$^{+/-}$ and *Gpr44* KO mice had no effect on WIHN; n = 8–12. Similar to 4b, *Gpr44* KO mice demonstrate increased WIHN compared to *Gpr44*$^{+/-}$ mice.